Inorg. Chem. **2007**, *46*, 7998–8007

Adventures in Crystallization. Crystalline Salts Containing One, Two, or Even Three Chemically Distinct Cations Obtained from Solutions of $[(\text{Cyclohexyl Isocyanide})_4\text{Rh}^{\text{I}}]^+$

Ngon T. Tran, Jay R. Stork, David Pham, Christopher J. Chancellor, Marilyn M. Olmstead, James C. Fettinger, and Alan L. Balch*

Department of Chemistry, University of California, Davis, California 95616

Received April 26, 2007

By judicious selection of crystallization conditions, it has been possible to obtain the salts of a common building block, $[(RNC)_4Rh^{I}]^+$, in single-crystal form suitable for X-ray diffraction. Salts that contain a single type of cation include deep green $[(C_6H_{11}NC)_{12}Rh^{I}_3](SbF_6)_3$, deep green $[(C_6H_{11}NC)_{12}Rh^{I}_3](AsF_6)_3$, and straw yellow $[(C_6H_{11}NC)_8Rh^{II}_2Cl_2](BF_4)_2$ (in addition to the previously isolated trimeric deep green $[(i\text{-PrNC})_{12}Rh^{I}_3]Cl_3\cdot 4.5H_2O$, monomeric, $[(C_6H_{11}NC)_4\,Rh^{I}](BPh_4)$, and $[(i\text{-PrNC})_4Rh^{I}](BPh_4)$ (both yellow), and red, dimeric $[(C_6H_{11}NC)_8Rh^{I}_2]Cl_2\cdot 0.5C_6H_6\cdot 2H_2O$). Ordered crystals of $[(C_6H_{11}NC)_{12}Rh^{I}_3](SbF_6)_3$ contain linear Rh_3 units, while those of $[(C_6H_{11}NC)_{12}Rh^{I}_3](AsF_6)_3$ show disorder which is consistent with the presence of linear or bent Rh_3 units. The formation of green $[(C_6H_{11}NC)_{12}Rh^{V/III}_3Cl_2][(C_6H_{11}NC)_{12}Rh^{I}_3]Cl_6$, and brown $[(C_6H_{11}NC)_{12}Rh^{V/III}_3Cl_2][(C_6H_{11}NC)_8Rh^{I}_2][(C_6H_{11}NC)_4Rh^{I}]Cl_6\cdot 16H_2O\cdot 3C_6H_6$ along with unidentified red-brown cubes from an air-exposed solution of $[(C_6H_{11}NC)_4Rh^{I}]Cl$ is reported. As their formulas indicate, green $[(C_6H_{11}NC)_{12}Rh^{V/III}_3Cl_2][(C_6H_{11}NC)_{12}Rh^{I}_3]Cl_6$, and brown $[(C_6H_{11}NC)_{12}Rh^{V/III}_3Cl_2][(C_6H_{11}NC)_8Rh^{I}_2][(C_6H_{11}NC)_8Rh^{I}]Cl_6\cdot 16H_2O\cdot 3C_6H_6$ contain two or three chemically distinct cations, respectively, but again are built from a common precursor, $[(C_6H_{11}NC)_4Rh^{I}]^+$.

Introduction

Direct metallophilic interactions between closed-shell d^{10} and between pseudo-closed-shell d^8 transition metal complexes are well known, particularly in crystalline solids where dimers, trimers, and extended chains readily form. Thus, many planar, d^8 complexes crystallize to form linear or nearly linear chains of metal ions. For example, Magnus' green salt, $[(NH_3)_4Pt][PtCl_4]$, contains linear columns in which the cations and anions alternate to form weak Pt−Pt interactions.[1] Prominent examples of self-association of d^8 Pt(II) complexes include numerous salts of $[Pt^{II}(CN)_4]^{2-}$ [2] and $[Pt^{II}(ox)_2]^{2-}$,[3] as well as neutral molecules like (2,2′-bipyridine)$Pt^{II}Cl_2$.[4−6] Similar extended chains of linear, two-coordinate d^{10} complexes of Au^{I} also occur when they crystallize. Examples here include the salts of $[(C_6H_{11}NC)_2Au^{I}]^+$ [7] and $[\{(MeHN)_2C\}_2Au^{I}]^+$ [8] and the neutral molecules (RNC)Au^{I}X with X = Cl, Br, I, and CN.[9,10]

The Rh^{I} cations $[(RNC)_4Rh^{I}]^+$, where R may be an alkyl group or an aryl group, present a system that is unusually amenable for the study of self-association not only in the solid state but in solution as well.[11] Monomeric $[(RNC)_4Rh^{I}]^+$ is readily recognized by its yellow color, while the oligomeric forms are red, blue, or green. In solution these different

* To whom correspondence should be addressed. E-mail: albalch@ucdavis.edu.

(1) Caseri, W. R.; Chanzy, H. D.; Feldman, K.; Fontana, M.; Smith, P.; Tervoort, T. A.; Goossens, J. G. P.; Meijer, E. W.; Schenning, A. P. H. J.; Dolbyna, I. P.; Debije, M. G.; de Haas, M. P.; Warman, J. M.; van de Craats, A. M.; Friend, R. H.; Sirringhaus, H.; Stutzmann, N. *Adv. Mater*. **2003**, *15*, 125.
(2) Williams, J. M.; Schultz, A. J.; Underhill, A. E.; Carneiro, K. In *Extended Linear Chain Compounds*; Miller, J. S., Ed.; Plenum Press: New York, 1982; Vol. 1, p 73.
(3) Underhill, A. E.; Watkins, D. M.; Williams, J. M.; Carneiro, K. In *Extended Linear Chain Compounds*; Miller, J. S., Ed.; Plenum Press: New York, 1982; Vol. 1, p 119.
(4) Osborn, R. S.; Rogers, D. *J. Chem. Soc., Dalton Trans*. **1974**, 1002.
(5) Achar, S.; Catalano, V. J. *Polyhedron* **1997**, *16*, 1555.
(6) Grzesiak, A. L.; Matzger, A. J. *Inorg. Chem*. **2007**, *46*, 453.
(7) White-Morris, R. L.; Olmstead, M. M.; Balch, A. L. *J. Am. Chem. Soc*. **2003**, *125*, 1033.
(8) White-Morris, R. L.; Olmstead, M. M.; Jiang, F.; Tinti, D. S.; Balch, A. L. *J. Am. Chem. Soc*. **2002**, *124*, 2327.
(9) White-Morris, R. L.; Olmstead, M. M.; Balch, A. L.; Elbjeirami, O.; Omary, M. A. *Inorg. Chem*. **2003**, *42*, 6741.
(10) White-Morris, R. L.; Stender, M.; Tinti, D. S.; Balch, A. L. *Inorg. Chem*. **2003**, *42*, 3237.
(11) Mann, K. R.; Gordon, J. G., II; Gray, H. B. *J. Am. Chem. Soc*. **1975**, *97*, 3553.

10.1021/ic7008013 CCC: $37.00
Published on Web 08/15/2007

Scheme 1. Equilibria Involving Self-Association

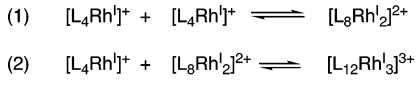

Scheme 2. Equilibria Involving Oxidative Addition

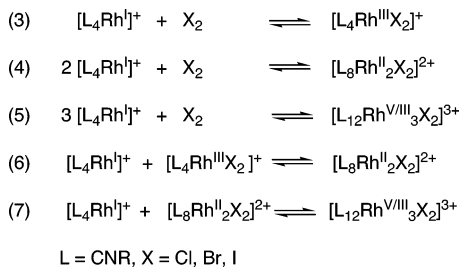

species are related by the equilibria shown in Scheme 1. These equilibria have been examined extensively for the case where R = Ph, and the equilibrium constants K(eq 1) = 35 and K(eq 2) = ~10 obtained for acetonitrile solution at 25 °C.[12] The monomeric yellow complex can be obtained in crystalline form by utilizing bulky R substituents to eliminate self-association.[13] A number of salts containing dimeric dications, $[(RNC)_8Rh^I_2]^{2+}$, have been isolated and crystallographically characterized. Such cations generally have Rh−Rh separations of about 3.2 Å (3.193(1) Å for $[(PhNC)_8Rh^I_2](BPh_4)_2$,[12] 3.207(2) Å for $[(p\text{-}FC_6H_4NC)_8Rh^I_2]Cl_2\cdot H_2O$,[14] and 3.25(1) Å for $[(p\text{-}O_2NC_6H_4NC)_8Rh^I_2]Cl_2$[14]). Recently, this laboratory reported that variation in the conditions used for crystallization including changes in anion and solvent allowed the isolation of crystalline samples of $[(RNC)_4Rh^I]^+$ (R = *i*-Pr or C_6H_{11}) in monomeric, dimeric, or trimeric forms.[15] The trimer was bent, and the Rh−Rh separation in the trimer was shorter than the Rh−Rh separation in the dimer.

These cations also undergo oxidative addition reactions that lead to the formation of a further set of oligomeric cations, as seen in Scheme 2. In addition to the normal one-center, two-electron oxidative addition to give the Rh(III) product seen in eq 3, $[(RNC)_4Rh^I]^+$ also undergoes two-center, two-electron oxidation to form a Rh(II) dimer, as shown in eq 4,[16,17] and three-center, two-electron oxidation to form the fractionally oxidized trinuclear complex shown in eq 5.[18] Further equilibria involving $[(RNC)_4Rh^{III}X_2]^+$ as oxidant also occur as shown by eq 6 and 7. The dimeric Rh(II) cation, $[(p\text{-}CH_3C_6H_4NC)_8Rh^{II}_2I_2]^{2+}$, has been isolated as the hexafluorophosphate salt and shown to be connected by a two-electron, two-center Rh−Rh bond.[19] The Rh−Rh bond length (2.785(2) Å) in the Rh(II) dimer is shorter than the Rh−Rh distance of ca. 3.2 Å found in the related Rh(I) dimers. Similarly, the trinuclear cation, $[(C_6H_5CH_2NC)_{12}Rh^{V/III}_3I_2]^{3+}$, has been isolated as the bromide salt.[18] The cation is centrosymmetric and has a Rh−Rh bond length of 2.761 Å.

The present work was undertaken as part of our studies of self-association of d^{10} and d^8 metal complexes in the solid state. Frequently, we have found that different crystalline forms of these complexes show significant variations in the mode of self-association. This comment is particularly relevant in the case of polymorphs of linear, two-coordinate gold(I)[7,20] but also extends to polymorphs of d^8 complexes as well.[6,21] In regard to the rhodium(I) complexes that are the subject of this article, our initial goal was to crystallize the trimeric form of the cation, a form which had not been isolated previously, and to determine whether any other aggregates of $[L_4Rh^I]^+$ could be obtained in the solid state. Many self-associate to form extended chains of metal ions bond by metallophilic interactions, and we were curious to see whether $\{L_4Rh^I\}^+$ might also form an extended chain. We achieved our initial goal with the isolation of $[(i\text{-}PrNC)_{12}Rh^I_3]Cl_3\cdot 4.5H_2O$,[15] but in the process, we observed that several other crystalline materials could be obtained from solutions of $[(C_6H_{11}NC)_4Rh^I]^+$, some of which contained two or three chemically distinct cations in the same crystal. The isolation and structural characterization of these new salts are reported here.

Results

Isolation of Crystals Containing a Single Cation. In addition to the recently reported isolation of yellow crystals of monomeric cations, $[(C_6H_{11}NC)_4Rh^I](BPh_4)$ and $[(i\text{-}PrNC)_4Rh^I](BPh_4)$, the red dimeric complex, $[(C_6H_{11}NC)_8Rh^I_2]Cl_2\cdot 0.5C_6H_6\cdot 2H_2O$, and the green trimeric compound, $[(i\text{-}PrNC)_{12}Rh^I_3]Cl_3\cdot 4.5H_2O$,[15] we have been able to isolate two different examples of the trimeric cation, $[(C_6H_{11})_{12}Rh^I_3]^{3+}$, and the Rh(II) dimer, $[(C_6H_{11}NC)_8Rh^{II}_2Cl_2](BF_4)_2$, in single-crystal form. Green crystals of $[(C_6H_{11}NC)_{12}Rh^I_3](AsF_6)_3$ and $[(C_6H_{11}NC)_{12}Rh^I_3](SbF_6)_3$ were obtained by simple recrystallization of the salts, while straw yellow $[(C_6H_{11}NC)_8Rh^{II}_2Cl_2](BF_4)_2$ was obtained by aerial oxidation of $[(C_6H_{11}NC)_4Rh^I]Cl$.

Structure of Deep Green $[(C_6H_{11}NC)_{12}Rh^I_3](SbF_6)_3$. Green crystals of $[(C_6H_{11}NC)_{12}Rh^I_3](SbF_6)_3$ were obtained by slow cooling and evaporation of an ethanol solution of the salt. The structure of the trimeric cation is shown in Figure 1. Part A shows a view of the entire cation, while part B shows a drawing that emphasizes the staggered relationship of the ligands on adjacent rhodium ions and gives some of the labeling of the atoms. The middle rhodium ion, Rh1, of the trimer is located on a center of symmetry. Selected distances and angles within the cation are given in Table 1. The Rh1−Rh2 distance is rather short (vide infra) at 3.044(3) Å, and the Rh2−Rh1−Rh2A angle is required by symmetry to be 180°. The ligands connected to Rh2 in $[(C_6H_{11}NC)_{12}Rh^I_3](SbF_6)_3$ have the isocyanide groups in axial

(12) Mann, K. R.; Lewis, N. S.; Williams, R. M.; Gray, H. B.; Gordon, II, J. G. *Inorg. Chem.* **1978**, *17*, 828.
(13) Ashworth, T. V.; Liles, D. C.; Oosthuizen, H. E.; Singleton, E. *Acta Crystallogr., Sect. C* **1984**, *40*, 1169.
(14) Endres, H.; Gottstein, N.; Keller, H. J.; Martin, R.; Rodemer, W.; Steiger, W. *Z. Naturforsch., B: Chem. Sci.* **1979**, *34*, 827.
(15) Tran, N.; Stork, J. R.; Pham, D.; Olmstead, M. M.; Fettinger, J. C.; Balch, A. L. *Chem. Commun*. **2006**, 1130.
(16) Balch, A. L.; Olmstead, M. M. *J. Am. Chem. Soc*. **1976**, *98*, 2354.
(17) Olmstead, M. M.; Balch, A. L. *J. Organomet. Chem*. **1978**, *148*, C15.
(18) Balch, A. L.; Olmstead, M. M. *J. Am. Chem. Soc*. **1979**, *101*, 3128.
(19) Olmstead, M. M.; Balch, A. L. *J. Organomet. Chem*. **1978**, *148*, C15.
(20) White-Morris, R. L.; Olmstead, M. M.; Attar, S.; Balch, A. L. *Inorg. Chem*. **2005**, *44*, 5021.
(21) Stork, J. R.; Olmstead, M. M.; Balch, A. L. *J. Am. Chem. Soc*. **2005**, *127*, 6512.

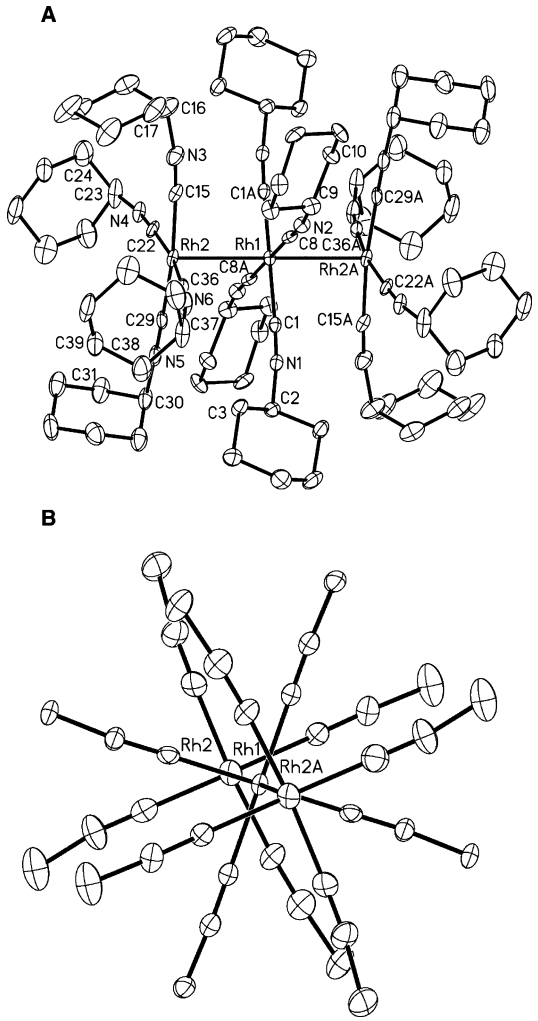

Figure 1. (A) Side view of the cation in deep green $[(C_6H_{11}NC)_{12}Rh^I_3](SbF_6)_3$ with 35% thermal contours. (B) A drawing of the cation in deep green $[(C_6H_{11}NC)_{12}Rh^I_3](SbF_6)_3$ looking down the Rh_3 axis with the cyclohexyl groups removed for clarity.

positions of the cyclohexyl ring and are arranged to form a cavity that surrounds the otherwise exposed surface of Rh2. The ligands attached to Rh1 have the isocyanide substituents in equatorial positions of the cyclohexyl ring. These groups protrude axially from Rh1 so that interactions with the ligands above and below are minimized.

Structure of Deep Green $[(C_6H_{11}NC)_{12}Rh^I_3](AsF_6)_3$. Green crystals of $[(C_6H_{11}NC)_{12}Rh^I_3](AsF_6)_3$ form in the same space group as the corresponding $(SbF_6)^-$ salt and have similar cell dimensions, as the crystal data in Table 2 show. However, the structure of the cation in $[(C_6H_{11}NC)_{12}Rh^I_3](AsF_6)_3$ differs slightly from that in $[(C_6H_{11}NC)_{12}Rh^I_3](SbF_6)_3$. The cation in $[(C_6H_{11}NC)_{12}Rh^I_3](AsF_6)_3$ is disordered with two equally populated positions for Rh2 (Rh2 and Rh2A) while Rh1 resides on a center of symmetry. Thus, there are two possible structures for the cation that need to be considered, as shown in Figure 2. In one situation, the Rh−Rh−Rh unit is linear and disordered over two orientations with Rh2 and its centrosymmetrically related counterpart Rh2′ as the terminal rhodium ions. In the other, the Rh−Rh−Rh unit is bent at an angle of 175.40(17)° and the cation is disordered utilizing Rh2 for one of the terminal rhodium ions and the non-centrosymmetrically related Rh2A for the other. It is also possible that both the bent and the linear arrangements are present in the crystal, again in a disordered fashion. Unfortunately, the available crystallographic data do not allow us to differentiate between these possibilities. The Rh1−Rh2 and Rh1−Rh2A distances are again rather short: 3.040(3) and 3.044(3) Å, respectively. Other selected interatomic distances and angles for $[(C_6H_{11}NC)_{12}Rh^I_3](AsF_6)_3$ are given in Table 2. We have examined the structure of $[(C_6H_{11}NC)_{12}Rh^I_3](SbF_6)_3$ to determine whether it suffers from a similar form of disorder, but have concluded that the ordered model with only the linear Rh−Rh−Rh group is correct.

The Rh−Rh−Rh angle in the trinuclear cations varies from 168.05(2)° in $[(i\text{-}PrNC)_{12}Rh^I_3]Cl_3\cdot 4.5H_2O$ to 180° in $[(C_6H_{11}NC)_{12}Rh^I_3](SbF_6)_3$, while in $[(C_6H_{11}NC)_{12}Rh^I_3](AsF_6)_3$ it may be 180° or 175.40(17)°. The observations suggest that the Rh−Rh−Rh angle is easily bent and is subject to variation induced by crystal packing forces.

Structure of Straw Yellow $[(C_6H_{11}NC)_8Rh^{II}_2Cl_2](BF_4)_2$. Crystals of $[(C_6H_{11}NC)_8Rh^{II}_2Cl_2](BF_4)_2$ were obtained by allowing an aqueous solution of $[(C_6H_{11}NC)_4Rh^I]Cl$ and $(NH_4)_2SnF_6$ to stir in air for an hour with the expectation that an $(SnF_6)^{2-}$ salt of the rhodium cation would precipitate. It did not, and an aqueous solution of NH_4BF_4 was subsequently added. At this stage, straw yellow crystals of $[(C_6H_{11}NC)_8Rh^{II}_2Cl_2](BF_4)_2$ formed. The role of $(NH_4)_2SnF_6$ in this process is unclear, but is necessary for the procedure to succeed. If the $(NH_4)_2SnF_6$ is omitted, no $[(C_6H_{11}NC)_8Rh^{II}_2Cl_2](BF_4)_2$ forms when NH_4BF_4 is added.

The dimeric cation in $[(C_6H_{11}NC)_8Rh^{II}_2Cl_2](BF_4)_2$ has no crystallographically imposed symmetry. Figure 3 shows a view of this cation. The Rh−Rh distance, 2.6944(3) Å, is shorter than the corresponding Rh−Rh distance, 3.287(2) Å, in $[(C_6H_{11}NC)_8Rh^I_2]Cl_2\cdot 0.5C_6H_6\cdot 2H_2O$.[15] This bond shortening is consistent with oxidation. The isocyanide ligands on the two rhodium ions in $[(C_6H_{11}NC)_8Rh^{II}_2Cl_2](BF_4)_2$ are arranged in a staggered array, whereas in $[(C_6H_{11}NC)_8Rh^I_2]^{2+}$ these ligands are almost eclipsed.[15] However, in both dimers, all the isocyanide substituents are in axial positions of the cyclohexyl rings and these rings are oriented to minimize interaction with one another.

Isolation of Three Different Types of Crystals (Red-Orange Cubes, Green Plates, and Brown Plates) from a Single Solution. Slow diffusion of moist diethyl ether or cyclohexane into a benzene solution of $[(C_6H_{11}NC)_4Rh^I]Cl$ with no protection from atmospheric air and water results in the formation of three different types of crystals. Green plates grew in the diethyl ether or cyclohexane layer, large cubes of red-orange crystals grew in the benzene phase, and brown plates developed at the interface between the two liquids. The green crystals that formed in the ether or cyclohexane phase were a lighter shade of green than the crystals of $[(C_6H_{11}NC)_{12}Rh^I_3](SbF_6)_3$ or $[(C_6H_{11}NC)_{12}Rh^I_3](AsF_6)_3$ discussed in the previous sections. Crystallographic analysis of these lighter green crystals ($[(C_6H_{11}NC)_{12}Rh^I_3][(C_6H_{11}NC)_{12}Rh^{V/III}_3Cl_2]Cl_6$) revealed that they contain two different cations: a trimer, $[(C_6H_{11}NC)_{12}Rh^I_3]^{3+}$, which is

Table 1. Crystallographic Data

	$[(C_6H_{11}NC)_{12}Rh^{I}_3]$ $(SbF_6)_3$	$[(C_6H_{11}NC)_{12}Rh^{I}_3]$ $(AsF_6)_3$	$[(C_6H_{11}NC)_8Rh^{II}_2Cl_2]$ $(BF_4)_2$
color/habit	green plate	green block	pale yellow plate
formula	$C_{84}H_{132}F_{18}N_{12}Rh_3Sb_3$	$C_{84}H_{132}As_3F_{18}N_{12}Rh_3$	$C_{56}H_{88}B_2Cl_2F_8N_8Rh_2$
fw	2326.00	2185.51	1323.68
cryst syst	triclinic	triclinic	triclinic
space group	$P\bar{1}$	$P\bar{1}$	$P\bar{1}$
a, Å	14.177(3)	14.1370(15)	12.1642(7)
b, Å	14.824(5)	14.5845(15)	13.3121(7)
c, Å	14.954(4)	14.9187(15)	20.4320(11)
α, deg	114.690(5)	114.214(2)	87.576(3)°
β, deg	118.171(3)	118.089(2)	82.919(3)°
γ, deg	89.940(4)	90.083(2)	74.413(3)°
V, Å^3	2440.4(12)	2401.5(4)	3162.4(3)
Z	1	1	2
T, K	90(2)	90(2)	90(2)
λ, Å	0.71073	0.71073	0.71073
D, g/cm^3	1.583	1.511	1.390
μ, mm^{-1}	1.395	1.617	0.671
R1 (obsd data)[a]	0.050	0.042	0.0422
wR2 (all data)[b]	0.147	0.111	0.1060
	$[(C_6H_{11}NC)_{12}Rh^{V/III}_3Cl_2]$ $[(C_6H_{11}NC)_{12}Rh^{I}_3]Cl_6$	$[(C_6H_{11}NC)_{12}Rh^{V/III}_3Cl_2]$ $[(C_6H_{11}NC)_8Rh^{I}_2]$ $[(C_6H_{11}NC)_4RH^{I}]Cl_6 \cdot 16H_2O \cdot 3C_6H_6$	
color/habit	green plate	brown plate	
formula	$C_{168}H_{264}Cl_8N_{24}Rh_6$	$C_{186}H_{314}Cl_6N_{24}O_{16}Rh_6$	
fw	3521.09	3972.78	
cryst syst	triclinic	monoclinic	
space group	$P\bar{1}$	$P2_1/c$	
a, Å	13.8444(8)	21.101(4)	
b, Å	16.0352(9)	20.105(3)	
c, Å	21.3744(12)	23.857(4)	
α, deg	92.785(2)	90	
β, deg	91.905(2)	91.086(4)	
γ, deg	111.914(2)	90	
V, Å^3	4390.2(4)	10119(3)	
Z	1	2	
T, K	90(2)	90(2)	
λ, Å	0.71073	0.71073	
D, g/cm^3	1.332	1.304	
μ, mm^{-1}	0.727	0.619	
R1 (obsd data)	0.065	0.123	
wR2 (all data)	0.188	0.349	

[a] For data with $I > 2\sigma I$, $(\sum||F_o| - |F_c||)/\sum|F_o|$. [b] For all data, wR2 $= \sqrt{(\sum[w(F_o^2-F_c^2)^2])/\sum[w(F_o^2)^2]}$.

similar to the cations found in $[(C_6H_{11}NC)_{12}Rh^{I}_3](AsF_6)_3$ and $[(C_6H_{11}NC)_{12}Rh^{I}_3](SbF_6)_3$, and an oxidized trinuclear complex, $[(C_6H_{11}NC)_{12}Rh^{V/III}_3Cl_2]^{3+}$. A crystal structure determination of the brown plates ($[(C_6H_{11}NC)_{12}Rh^{V/III}_3Cl_2][(C_6H_{11}NC)_8Rh^{I}_2][(C_6H_{11}NC)_4Rh^{I}]Cl_6 \cdot 16H_2O \cdot 3C_6H_6$) shows that they consist of three different rhodium containing cations: monomeric $[(C_6H_{11}NC)_4Rh^{I}]^+$, dimeric $[(C_6H_{11}NC)_8Rh^{I}_2]^{2+}$, and the trinuclear, partially oxidized $[(C_6H_{11}NC)_{12}Rh^{V/III}_3Cl_2]^{3+}$. Despite considerable effort, no satisfactory solution to the structure of the red-orange cubes could be obtained.

Structure of Green $[(C_6H_{11}NC)_{12}Rh^{I}_3][(C_6H_{11}NC)_{12}Rh^{V/III}_3Cl_2]Cl_6$. The asymmetric unit consists of one-half of each of two different trinuclear cations and anions. Figure 4 shows a drawing of the cation, $[(C_6H_{11}NC)_{12}Rh^{I}_3]^{3+}$, in $[(C_6H_{11}NC)_{12}Rh^{I}_3][(C_6H_{11}NC)_{12}Rh^{V/III}_3Cl_2]Cl_6$. This cation is situated so that the central atom Rh4 resides at a center of symmetry. Again the Rh3−Rh4 distance is rather short, 3.0211(6) Å, and the Rh3−Rh4−Rh3A angle is required by symmetry to be 180°. Overall, the three cations in $[(C_6H_{11}NC)_{12}Rh^{I}_3](SbF_6)_3$, $[(C_6H_{11}NC)_{12}Rh^{I}_3](AsF_6)_3$, and $[(C_6H_{11}NC)_{12}Rh^{I}_3][(C_6H_{11}NC)_{12}Rh^{V/III}_3Cl_2]Cl_6$ are very similar. However, in the last of these compounds, the Rh3−Rh4 bond is more nearly perpendicular to the RhC_4 planes. The relevant angles are Rh3−Rh4 to the normal to the $Rh3C_4$ plane, 3.8°, Rh3−Rh4 to the normal to the $Rh4C_4$ plane, 8.1°. Additionally, in $[(C_6H_{11}NC)_{12}Rh^{I}_3][(C_6H_{11}NC)_{12}Rh^{V/III}_3Cl_2]Cl_6$, one of the cyclohexyl groups surrounding Rh3 has the isocyanide substituent in an equatorial position, otherwise the positions of the cyclohexyl groups in all three of these cations are similar.

Figure 4 also shows a drawing of the other cation in $[(C_6H_{11}NC)_{12}Rh^{I}_3][(C_6H_{11}NC)_{12}Rh^{V/III}_3Cl_2]Cl_6$. The ion $[(C_6H_{11}NC)_{12}Rh^{V/III}_3Cl_2]^{3+}$ retains the basic shape of the $[(C_6H_{11}NC)_{12}Rh^{I}_3]^{3+}$ cation but has two chloride ligands attached at each end of the Rh_3 chain. Again, the central rhodium ion in this cation resides at a center of symmetry. As expected for such a partially oxidized complex, the Rh1−Rh2 distance, 2.7626(5) Å, is shorter than the corresponding distances observed here for the Rh^{I} cation, $[(C_6H_{11}NC)_{12}Rh^{I}_3]^{3+}$. For comparison, the Rh−Rh distance in centrosymmetric $[(PhCH_2NC)_{12}Rh^{V/III}_3I_2]Br_3$ is 2.761(1) Å.[18]

The relationship between the two cations as they are situated in the crystal is shown in Figure 5. While the central rhodium ion in each cation is located at a center of symmetry,

Table 2. Selected Distances (Å) and Angles (deg) for Rhodium Cations

	$[(C_6H_{11}NC)_4Rh^I](BPh_4)$ [a]	$[(i\text{-}PrNC)_4Rh^I](BPh_4)$ [a]	$[(C_6H_{11}NC)_8Rh^I_2]Cl_2\cdot 0.5C_6H_6\cdot 2H_2O$ [a]	$[(i\text{-}PrNC)_{12}Rh^I_3]Cl_3\cdot 4.5H_2O$ [a]
		Distances (Å)		
Rh1−Rh2	NA, 8.6390(7)[b]	NA 8.5228(6)	3.287(2)	3.1012(6)
Rh2−Rh3	NA	NA	NA	3.0739(6)
range Rh−C	1.964(4)−1.986(4)	1.9722(12)	1.893(13)−1.981(11)	1.946(6)−1.976(6)
range C≡N	1.143(5)−1.176(6)	1.1532(16)	1.147(2)−1.157(4)	1.137(7)−1.147(6)
		Angles (deg)		
C−Rh−C (cis)	89.28(16)−90.70(16)	90.003(1)	84.69(13)−96.37(10)	88.65(13)−91.07(12)
C−Rh−C (trans)	176.72(18)−178.98(19)	179.14(7)	168.44(14)−173.79(7)	170.3(2)−179.46(18)
Rh−C−N	177.7(4)−179.0(4)	179.12(12)	172.44(15)−178.59(15)	175.8(5)−179.5(6)
C≡N−C	171.8(4)−179.9(4)	177.72(13)	171.25(17)−179.39(19)	174.7(7)−178.6(6)
Rh1−Rh−Rh3	NA	NA	NA	168.049(18)

	$[(C_6H_{11}NC)_{12}Rh^I_3](SbF_6)_3$	$[(C_6H_{11}NC)_{12}Rh^I_3](AsF_6)_3$	$[(C_6H_{11}NC)_{12}Rh^I_3]^{3+}$ in $[(C_6H_{11}NC)_{12}Rh^I_3][(C_6H_{11}NC)_{12}Rh^{V/III}{}_3Cl_2]Cl_6$	$[(C_6H_{11}NC)_{12}Rh^{II/V}{}_3Cl_2]^{3+}$ in $[(C_6H_{11}NC_{12}Rh^I_3][(C_6H_{11}NC)_{12}Rh^{V/III}{}_3Cl_2]Cl_6$
		Distances (Å)		
Rh1−Rh2	3.0716(11)	3.044(3)	3.0211(6)	2.7627(5)
Rh2−Rh3	3.0716(11)[c]	3.044(3)[c]	3.0211(6)[c]	2.7627(5)[c]
range Rh−C	1.947(9)−1.980(9)	1.849(14)−2.081(14)	1.897(10)−1.981(8)	1.965(6)−1.996(6)
range C≡N	1.125(12)−1.158(11)	1.135(7)−1.178(16)	1.144(9)−1.149(8)	1.140(8)−1.153(8)
Rh−X	NA	NA	NA	2.4697(17)
		Angles (deg)		
C−Rh−C (cis)	87.6(4)−92.0(4)	86.0(5)−94.0(5)	88.0(3)−98.07(19)	86.3(2)−93.7(2)
C−Rh−C (trans)	171.4(3)−180	173.2(8)−180	164.9(8)−180	175.4(3)−180
Rh−C−N	176.6(9)−179.4(7)	174.5(13)−178.1(10)	173.5(6)−178.6(7)	171.2(7)−176.3(6)
C≡N−C	169.1(11)−172.4(8)	170.0(14)−177.6(15)	173.4(7)−178.7(7)	166.5(6)−173.3(8)
Rh1−Rh2···Rh3	180	180 or 175.40(17)	180	180
X−Rh1−Rh2	NA	NA	NA	178.23(5)

[a] Data from Tran, N.; Stork, J. R.; Pham, D.; Olmstead, M. M.; Fettinger, J. C.; Balch, A. L. *Chem. Commun.* **2006**, 1130. [b] NA = not applicable, nearest contact given. [c] Determined by symmetry.

the two Rh_3 chains have different alignments. There are no unusual contacts between the two ions, nor are there any unusual interactions between the anions and the cations.

Structure of Brown $[(C_6H_{11}NC)_{12}Rh^{V/III}{}_3Cl_2][(C_6H_{11}NC)_8Rh^I_2][(C_6H_{11}NC)_4Rh^I]Cl_6\cdot 16H_2O\cdot 3C_6H_6$. The brown crystals that grow at the interface between the anti-solvent and benzene layers in the crystallization of $[(C_6H_{11}NC)_4Rh^I]Cl$ consist of three different rhodium containing cations: monomeric $[(C_6H_{11}NC)_4Rh^I]^+$, dimeric $[(C_6H_{11}NC)_8Rh^I_2]^{2+}$, and trimeric, partially oxidized $[(C_6H_{11}NC)_{12}Rh^{V/III}{}_3Cl_2]^{3+}$. The relationship between these components is shown in Figure 6. There are no unusual contacts between these entities or between them and the solvate molecules.

Rh4 in the monomeric cation lies on a crystallographic center of symmetry. In this cation, the two crystallographically distinct isocyanide ligands have the cyano group positioned in an equatorial site of the cyclohexyl ring.

Figure 7 shows an expanded view of the dimeric ion, $[(C_6H_{11}NC)_8Rh^I_2]^{2+}$. The dimeric units are also built about a crystallographic center of symmetry. In this case, the center of symmetry lies between the two rhodium (Rh3 and Rh3A) ions that comprise the dimer. The Rh3−Rh3A separation is 3.281(2) Å. The isocyanide ligands on the two rhodium ions are in an eclipsed arrangement as they are in $[(C_6H_{11}NC)_8Rh^I_2]Cl_2\cdot 0.5C_6H_6\cdot 2H_2O$.[15] Each of the four independent isocyanide ligands has the isocyano substituent in an axial position in the respective cyclohexyl ring. This orientation positions the cyclohexyl substituents away from their counterparts on the adjacent half of the dimer.

The central rhodium ion of the partially oxidized, trimeric ion, $[(C_6H_{11}NC)_{12}Rh^{V/III}{}_3Cl_2]^{3+}$, also lies on a crystallographic center of symmetry. The Rh1−Rh2 distance in this trimer is 2.7496(10) Å, a value similar the Rh−Rh distance of 2.796(1) Å found in the related trimer, $[(C_6H_5CH_2NC)_{12}Rh^{V/III}{}_3I_2]^{3+}$. The isocyano groups on Rh2 are in equatorial positions of the cyclohexyl rings, while the isocyano groups are in axial positions of the cyclohexyl rings on the outer two rhodium ions (Rh1 and Rh1A). The staggered arrangement of the isocyanide ligands on adjacent rhodium ions and the positioning of isocyano groups on the cyclohexyl rings minimize contact between the individual ligands.

Spectroscopic Results on Crystals. The isocyanide stretching frequencies in the infrared spectra of these crystals have been examined and found to reflect the oxidation state of the rhodium ions, and to a much lesser extent, the state of aggregation of the basic $[(C_6H_{11}NC)_4Rh^I]^+$ unit. Monomeric $[(C_6H_{11}NC)_4Rh^I](BPh_4)$ shows a single ν(NC) at 2162 cm^{-1}, and its counterpart, $[(i\text{-}PrNC)_4Rh^I]BPh_4$, also has ν(NC) at 2162 cm^{-1}. Oligomeric forms show more than one ν(NC) absorption. Dimeric $[(C_6H_{11}NC)_8Rh^I_2]Cl_2\cdot 0.5C_6H_6\cdot 2H_2O$ shows ν(NC) at a strong band at 2165 cm^{-1} with a second absorption at 2207 cm^{-1}. Trimeric $[(C_6H_{11}NC)_{12}Rh^I_3](AsF_6)_3$ shows a strong peak at 2166 cm^{-1} with a medium-intensity peak at slightly higher energy, 2207 cm^{-1}. Similarly, $[(C_6H_{11}NC)_{12}Rh^I_3](SbF_6)_3$ has a strong absorption at 2206 cm^{-1} and a medium-intensity band at 2171 cm^{-1}, while

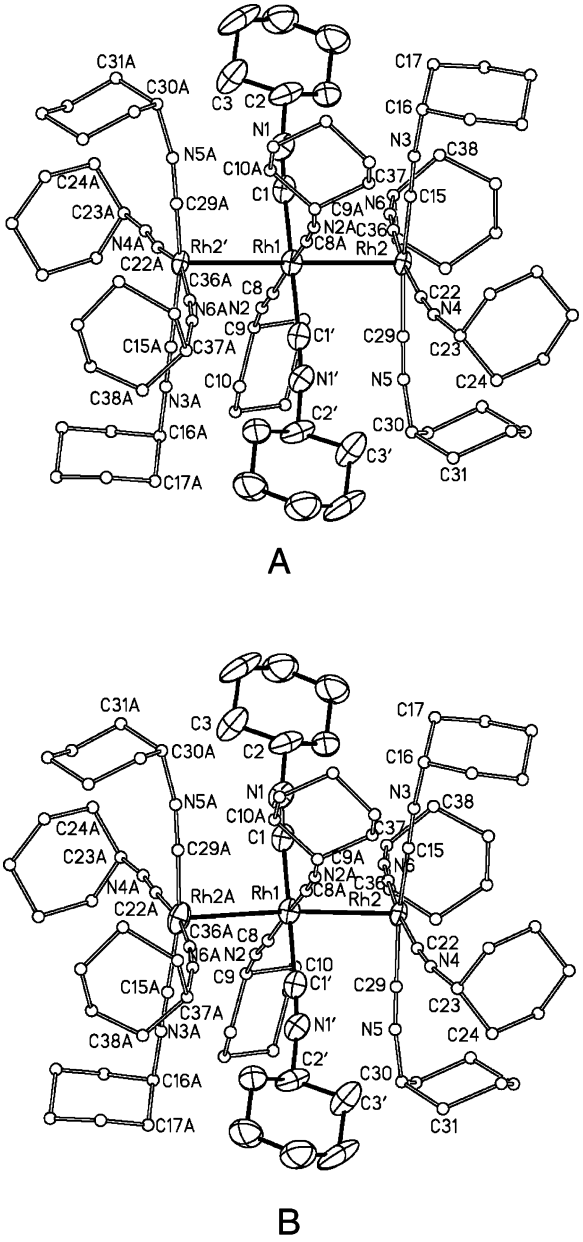

Figure 2. Drawings of the cation in deep green $[(C_6H_{11}NC)_{12}Rh^{I}_3](AsF_6)_3$ with 50% thermal contours for the anisotropically refined atoms and uniform, arbitrarily sized circles for the carbon atoms in the cyclohexyl rings that suffer from disorder. The disordered rings have two equally populated orientations, and all orientations are shown here with those labeled A belonging to the alternative set. (A) The linear structure. (B) The bent structure.

$[(i\text{-PrNC})_{12}Rh^{I}_3]Cl_3$ has strong band at 2207 cm^{-1} and a weak band at 2171 cm^{-1}.

As expected, oxidation of these rhodium(I) complexes results in an increase in ν(NC). Thus, $[(C_6H_{11}NC)_8Rh^{II}_2Cl_2](BF_4)_2$ shows ν(NC) at 2219 cm^{-1}.

For $[(C_6H_{11}NC)_{12}Rh^{I}_3][(C_6H_{11}NC)_{12}Rh^{V/III}_3Cl_2]Cl_6$, three bands are observed in the ν(NC) region, and these can be ascribed to the components present. Those at 2209 and 2168 cm^{-1} can be assigned to $[(C_6H_{11}NC)_{12}Rh^{I}_3]^{3+}$, while the remaining band at 2255 cm^{-1} is indicative of the presence of an oxidized complex and can be assigned to $[(C_6H_{11}NC)_{12}Rh^{V/III}_3Cl_2]^{3+}$. Crystals of $[(C_6H_{11}NC)_{12}Rh^{V/III}_3Cl_2][(C_6H_{11}NC)_8Rh^{I}_2][(C_6H_{11}NC)_4Rh^{I}]Cl_6\cdot16H_2O\cdot3C_6H_6$ decomposed too readily when taken from their mother liquor to allow us to obtain its infrared spectrum.

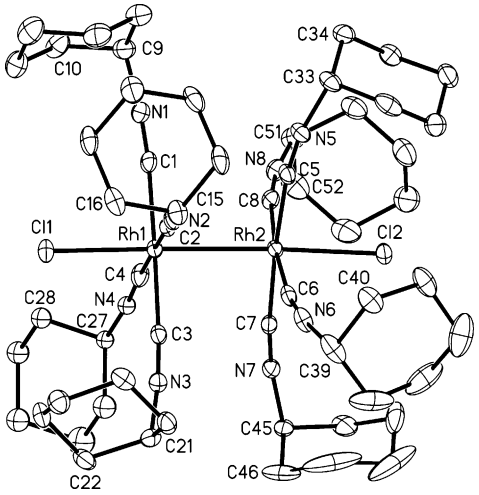

Figure 3. Drawing of the cation in straw yellow $[(C_6H_{11}NC)_8Rh^{II}_2Cl_2](BF_4)_2$ with 50% thermal contours.

The Uv/vis absorption spectra for samples of these crystalline complexes dispersed in KBr pellets are shown in Figure 8. Only the spectra of crystals containing one type of cation are included. The spectra of the monomeric, dimeric, and trimeric rhodium(I)-containing cations show a progression in the intense, low-energy absorption band to even lower energies as rhodium ions are added. A similar trend in the energy of this low-energy transition has been observed in the Uv/vis absorption spectra of solutions containing samples of $[(RNC)_4Rh^{I}]^+$ at various concentrations.[12] For example, aqueous solutions of $[(i\text{-PrNC})_4Rh^{I}]^+$ show a band at 383 nm for the monomer, a band at 495 nm for the dimer, and a band at 610 nm for the trimer.

These low-energy features are ascribed to a transition from a filled d_{z^2}-based molecular orbital to an empty p_z-based molecular orbital where the *z* axis is positioned perpendicular to the plane of the RhC_4 units. As rhodium ions are added to the aggregate, the separation between the filled d_{z^2} and the empty p_z molecular orbital decreases, as shown in the simplified molecular orbital diagram in Scheme 3.[12,15] This model predicts that the Rh−Rh bonding will strengthen in the excited state of the dimer. Appreciable bond length contraction in the excited state has been observed experimentally in such dinuclear rhodium(I) complexes.[22,23] The trimeric form should also show appreciable shortening of the Rh−Rh distances in the excited state.

Discussion

While crystallization is frequently considered a method for purification of solids, the crystalline product need not contain a single species, a situation exemplified here by the concomitant formation of $[(C_6H_{11}NC)_{12}Rh^{I}_3][(C_6H_{11}NC)_{12}Rh^{V/III}_3Cl_2]Cl_6$ and $[(C_6H_{11}NC)_{12}Rh^{V/III}_3Cl_2][(C_6H_{11}NC)_8Rh^{I}_2][(C_6H_{11}NC)_4Rh^{I}]Cl_6\cdot16H_2O\cdot3C_6H_6$. The formation of these

(22) Rice, S. F.; Gray, H. B. *J. Am. Chem. Soc.* **1981**, *103*, 1593.
(23) Coppens, P.; Gerlits, O.; Vorontsov, I. I.; Kovalevsky, A. Yu.; Chen, Y.-S.; Graber, T.; Gembocky, M.; Novozhilova, I. V. *Chem. Commun.* **2004**, 2144.

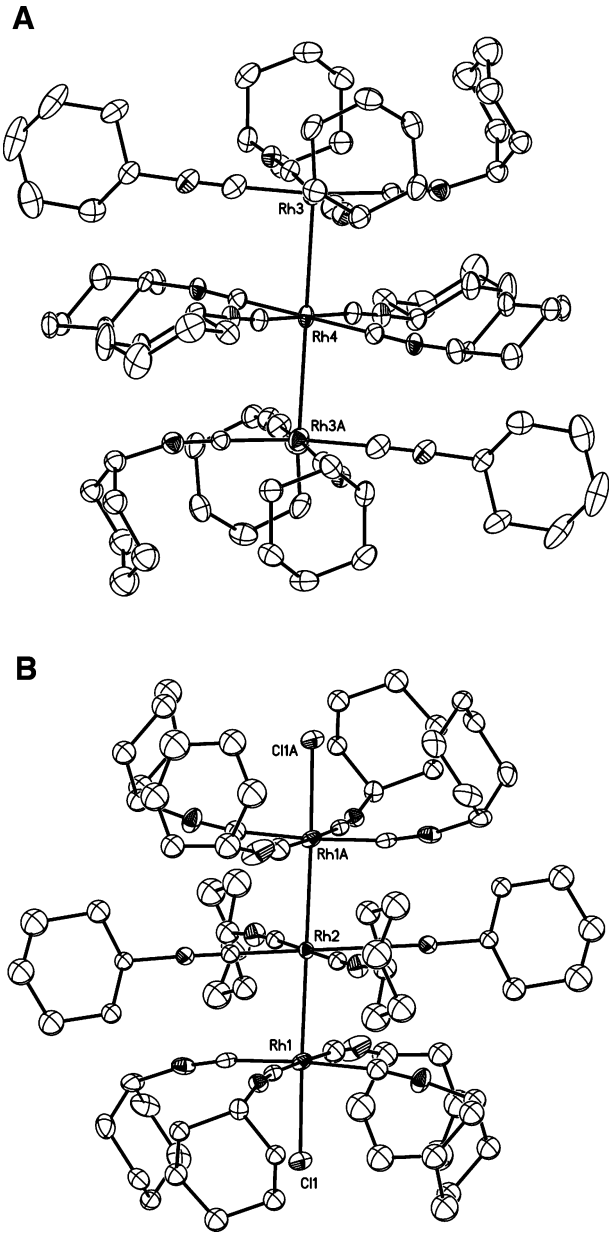

Figure 4. (A) View of the $[(C_6H_{11}NC)_{12}Rh^{I}_3]^{3+}$ cation in green $[(C_6H_{11}NC)_{12}Rh^{I}_3][(C_6H_{11}NC)_{12}Rh^{III/V}_3Cl_2]Cl_6$ with 50% thermal contours. (B) A drawing of the $[(C_6H_{11}NC)_{12}Rh^{III/V}_3Cl_2]^{3+}$ cation in the same salt with 50% thermal contours.

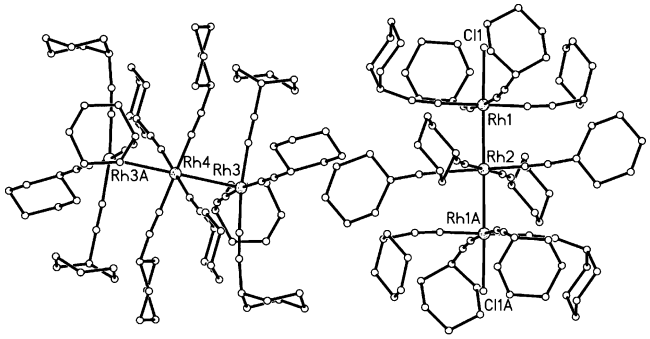

Figure 5. Drawing showing the relationship of the two cations in green $[(C_6H_{11}NC)_{12}Rh^{I}_3][(C_6H_{11}NC)_{12}Rh^{III/V}_3Cl_2]Cl_6$.

solids, which contain two or three chemically different cations, results from the occurrence of multiple equilibria in solution

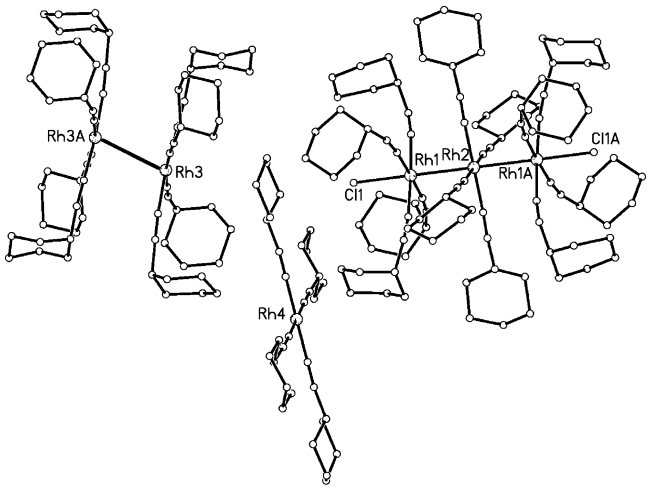

Figure 6. Drawing showing the relationship of the three cations in brown $[(C_6H_{11}NC)_{12}Rh^{V/III}_3Cl_2][(C_6H_{11}NC)_8Rh^{I}_2][(C_6H_{11}NC)_4Rh^{I}]Cl_6 \cdot 16H_2O \cdot 3C_6H_6$. For clarity, the atoms are shown as uniform, arbitrarily sized circles.

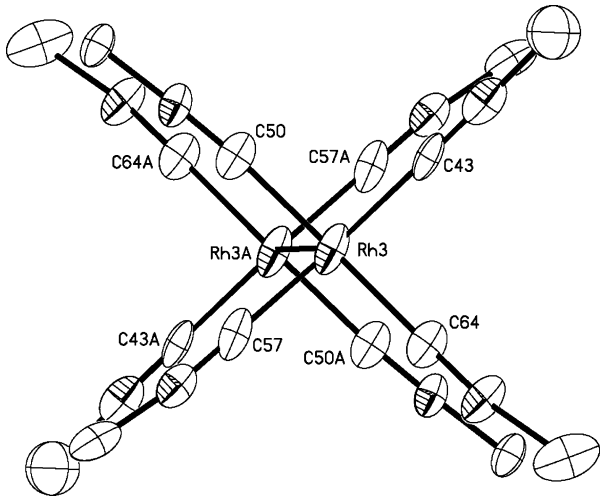

Figure 7. Drawing showing the eclipsed structure of the dimeric cation $[(C_6H_{11}NC)_8Rh^{I}_2]^{2+}$ in brown $[(C_6H_{11}NC)_{12}Rh^{V/III}_3Cl_2][(C_6H_{11}NC)_8Rh^{I}_2]$-$[(C_6H_{11}NC)_4Rh^{I}]Cl_6 \cdot 16H_2O \cdot 3C_6H_6$.

that allow the various components to coexist, nucleate, and crystallize. There are a number of other cases of crystals of transition metal complexes in which two different, chemically distinct forms are present. Perhaps the most immediately relevant example is the case of the copper(I) chloride complex of bis(diphenylphosphinothioyl)methane, $\{Ph_2P(S)CH_2PSPPh_2\}Cu^{I}Cl$, which crystallizes with a monomeric and a dimeric form in the same crystal.[24] The monomer has three-coordinate geometry, while the dimer is formed by linking two monomers through two additional Cu−S bonds, rather than the Rh−Rh bonds seen in the present study. Precedent for finding a crystal containing metal complexes in different oxidation states is found in the complex, $Ni^{III}Br_3(PMe_2Ph)_2 \cdot 0.5Ni^{II}Br_2(PMe_2Ph)_2 \cdot C_6H_6$.[25] In this case, a five-coordinate Ni(III) complex with trigonal bipyramidal geometry and a trans-planar Ni(II) complex are both present.

(24) Ainscough, E. W.; Brodie, A. M.; Brown, K. L. *J. Chem. Soc., Dalton Trans.* **1980**, 1042.
(25) Meek, D. W.; Alyea, E. C.; Stalick, J. K.; Ibers, J. A. *J. Am. Chem. Soc.* **1969**, *91*, 4920.

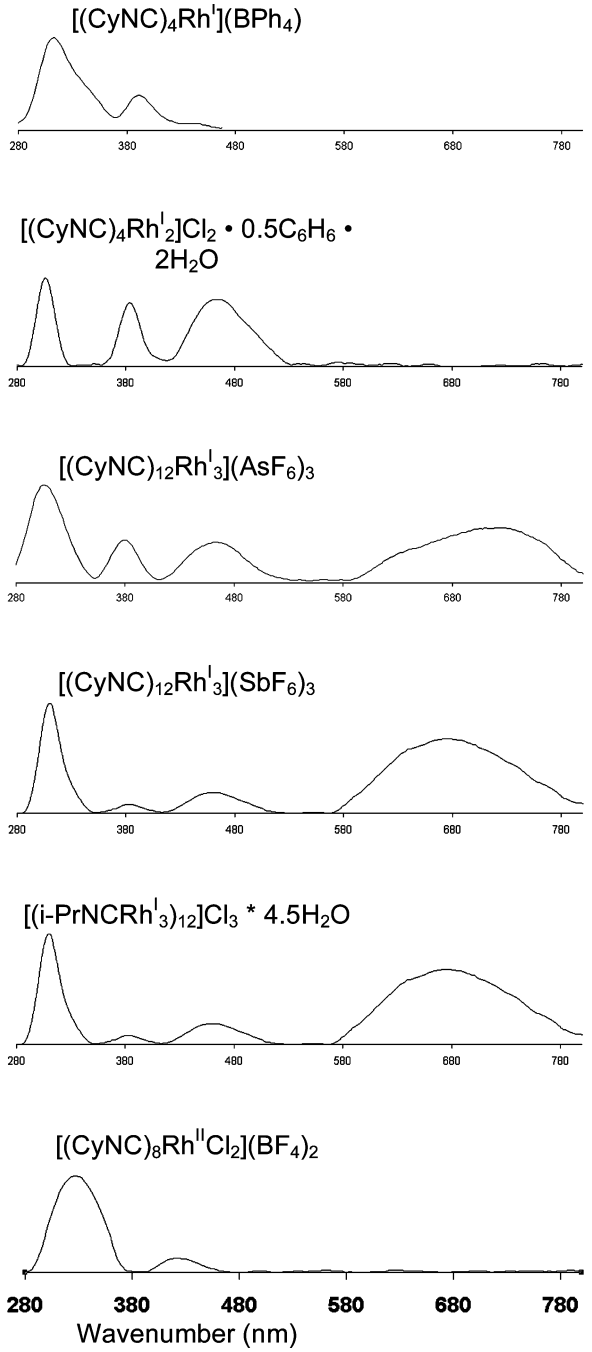

Figure 8. Uv/vis absorption spectra for polycrystalline samples of $[(C_6H_{11}NC)_4Rh^I](BPh_4)$, $[(C_6H_{11}NC)_8Rh^I_2]Cl_2 \cdot 0.5C_6H_6 \cdot 2H_2O$, $[(C_6H_{11}NC)_{12}Rh^I_3](AsF_6)_3$, $[(C_6H_{11}NC)_{12}Rh^I_3](SbF_6)_3$, $[(i\text{-}PrNC)_{12}Rh^I_3]Cl_3 \cdot 4.5H_2O$, and $[(C_6H_{11}NC)_8Rh^I_2Cl_2](BF_4)_2$.

Several cases where chemically different species are present in a single crystal involve cocrystallization of isomers where the two different isomeric forms are in rapid equilibrium in the solution used for crystal growth. For example, $[Cr^{III}(NH_2CH_2CH_2NH_2)_3][Ni^{II}(CN)_5] \cdot 1.5H_2O$ contains two different anions, one with square pyramidal coordination, the other with slightly distorted trigonal-bipyramidal geometry.[26] Similarly, $\{Ph_2(Ph_2CH_2)P\}_2Ni^{II}Br_2$ crystallizes with both tetrahedral and trans-planar forms of the complex in the same crystal. Five-coordinate $Ru(CO)_2\{P(i\text{-}Pr)_2Me\}_3$ crystallizes with two different isomers present.[27] One molecule has trigonal-bipyramidal geometry with the two carbon monoxide ligands in axial positions and a C_{3v} core, while the other has a Ru_2P_3 core with C_{2v} symmetry.[28] A somewhat different situation pertains to the yellow crystals of $Ni^{II}(stien)_2(O_2CCHCl_2)_2 \cdot [Ni^{II}(stien)_2](O_2CCHCl_2)_2 \cdot 2C_2H_5OH \cdot 4H_2O$ (where stien is *meso*-stilbenediamine). This type of crystal contains two distinct nickel(II) complexes with different coordination numbers: pseudo-octahedral molecules of $Ni^{II}(stien)_2(O_2CCHCl_2)_2$ along with planar, four-coordinate cations, $[Ni^{II}(stien)_2]^{2+}$.[29] Yet another situation pertains with the yellow-gold crystals of $(C_5Me_5)_2Y(\mu\text{-}Cl)_2Li(THF)_2 \cdot (C_5Me_5)_2Y(\mu\text{-}Cl)Li(THF)_3$, which contain molecules that differ by having one or two bridging chloride ligands and three or two molecules of THF coordinated to the lithium ions.[30] Three distinct copper complexes are present in the complex solid $\{(en)_2Cu^{II}(\mu\text{-}NC)NCCu^I(\mu\text{-}CN)_2Cu^ICN(\mu\text{-}CN)Cu^{II}(en)_2\}[Cu^{II}(en)_2]_2[Cu^I(CN)_3]_2 \cdot 2H_2O$.[31] Finally, we note an interesting case where a solution equilibrium between the green monomer (*N*,*N*′,*N*″-trimethyltriazacyclononane)$Cu^{II}Cl_2$ and yellow binuclear [{(*N*,*N*′,*N*″-trimethyltriazacyclononane)-Cu^{II}}$_2(\mu\text{-}Cl)_3$] produces composite crystals consisting of one green section and a second yellow section.[32]

The results presented here demonstrate that, with patience and care in adjusting the conditions for crystallization, it is possible to obtain crystalline samples of the basic $[(C_6H_{11}$-

Scheme 3. Simplified Molecular Orbital Diagram Showing the Interactions of the Out-of-Plane d_{z^2} and p_z Orbitals for $[(RNC)_4Rh]_n$ with D_{4h} Symmetry

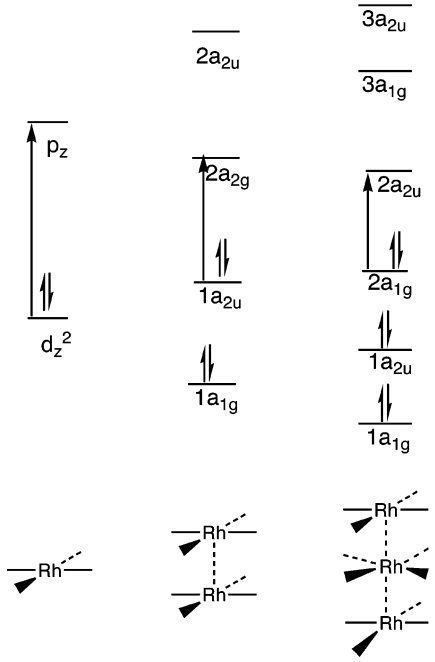

(26) Raymond, K. N.; Cornfield, P. W. R.; Ibers, J. A. *Inorg. Chem.* **1968**, *7*, 1362.

(27) Ogasawara, M.; Maseras, F.; Gallego-Planas, N.; Streib, W. E.; Eisenstein, O.; Caulton, K. G. *Inorg. Chem.* **1996**, *35*, 7468.
(28) Kilbourn, B. T.; Powell, H. M. *J. Chem. Soc. A* **1970**, 1688.
(29) Nyburg, S. C.; Wood, J. S. *Inorg. Chem.* **1964**, *3*, 468.
(30) Evans, W. J.; Boyle, T. J.; Ziller, J. W. *Inorg. Chem.* **1992**, *31*, 1120.
(31) Weiss, R.; Jansen, G.; Boese, R.; Epple, M. *Dalton Trans.* **2006**, 1831.
(32) Steed, J. W.; Goeta, A. E.; Lipowski, J.; Swierczynski, D.; Panteleon, V.; Handa, S. *Chem. Commun.* **2007**, 813.

$NC)_4Rh^I]^+$ unit in monomeric, dimeric, or trimeric form. No evidence has been found for the existence of extended chains of these cations in any of the crystalline solids discovered to date. Clearly, the anion plays a significant role in determining what form crystallizes. For example, only when a potential coordinating anion, chloride, is present have we observed that samples of $[(C_6H_{11}NC)_4Rh^I]^+$ are able to undergo oxidation in air. Thus, crystals of $[(C_6H_{11}NC)_8Rh^{II}_2Cl_2](BF_4)_2$ are obtained by stirring an aqueous solution of $[(C_6H_{11}NC)_4Rh^I]Cl$, $(NH_4)_2(SnF_6)$, and $(NH_4)(BF_4)$ in air and crystals of $[(C_6H_{11}NC)_{12}Rh^I_3][(C_6H_{11}NC)_{12}Rh^{V/III}_3Cl_2]Cl_6$ and $[(C_6H_{11}NC)_{12}Rh^{V/III}_3Cl_2][(C_6H_{11}NC)_8Rh^I_2][(C_6H_{11}NC)_4Rh^I]Cl_6 \cdot 16H_2O \cdot 3C_6H_6$, each of which contains one partially oxidized cation, were obtained by allowing a benzene solution of $[(C_6H_{11}NC)_4Rh^I]Cl$ to stir in air. In contrast, when the counterions are $(BPh_4)^-$, $(AsF_6)^-$, or $(SbF_6)^-$, rhodium(I)-containing crystals are formed, but in the case with $(BPh_4)^-$, a monomer crystallizes, while with $(AsF_6)^-$ or $(SbF_6)^-$ the trimer, $[(C_6H_{11}NC)_{12}Rh^I_3]^{3+}$, crystallizes. However, one should not expect that the anion alone determines which of the forms of the $[L_4Rh^I]^{+n}_n$ ions crystallize from a particular solution. The substituent on the isocyanide ligand and the solvent will also play roles in determining the solubility and nucleation rates for the various components. Thus, while crystallization with $(BPh_4)^-$ produced the monomer $[(C_6H_{11}NC)_4Rh^I](BPh_4)$ when cyclohexyl substituents were present,[15] dimeric $[(PhNC)_8Rh^I_2](BPh_4)_2$ formed when phenyl substituents were involved.[12] Finding the appropriate anion and solvent combination that allowed the formation of any particular aggregate of the $[(C_6H_{11}NC)_4Rh^I]^+$ unit required the examination of an array of experimental crystallization conditions.

In a different but related vein, we note that Dunbar and co-workers have reported a related family of acetonitrile complexes of rhodium in various oxidation states.[33] These complexes include $[(CH_3CN)_2(CO)_2Rh^I](BF_4)$, which contains an extended chain of rhodium ions with alternating Rh−Rh distances of 3.1528(14) Å and 3.1811(14) Å, $[(CH_3CN)_8Rh^{III/II}_2](BF_4)_3$, with an extended chain of rhodium centers and alternating Rh−Rh distances of 2.8442(8) and 2.9277(8) Å, $[(CH_3CN)_{10}Rh^{II}_2](BF_4)_2$, a dimer with a staggered geometry and a Rh−Rh distance of 2.624(1) Å, and $[(CH_3CN)_6Rh^{III}](BF_4)_3$, a six-coordinate monomer.

This work and related studies have resulted in several cases of the isolation of a particular type of ion in multiple different crystalline environments. Comparisons between these structural variants can be enlightening. For example, ions of the type $[(RNC)_{12}Rh^I_3]^{3+}$ are found in four different salts. In $[(i\text{-}PrNC)_{12}Rh^I_3]Cl_3 \cdot 4.5H_2O$, the trinuclear ion is bent with a Rh−Rh−Rh angle of 168.049(18)°, while in $[(C_6H_{11}NC)_{12}Rh^I_3](SbF_6)_3$ and $[(C_6H_{11}NC)_{12}Rh^I_3][(C_6H_{11}NC)_{12}Rh^{V/III}_3Cl_2]Cl_6$, the Rh_3 unit is linear. In $[(C_6H_{11}NC)_{12}Rh^I_3](AsF_6)_3$, either a bent or a linear arrangement of the three rhodium ions may be present since the structure is disordered. The variations observed here suggest that the Rh_3 unit is readily bent in $[(RNC)_{12}Rh^I_3]^{3+}$. However, despite the variations in degree of bending, in all four cases of ions of the type, $[(RNC)_{12}Rh^I_3]^{3+}$, the Rh−Rh separations fall in the narrow range 3.02−3.10 Å and are shorter than the Rh−Rh distances in the dimeric ions, $[(RNC)_8Rh^I_2]^{2+}$, which fall in the range 3.19−3.29 Å.[11−13] This shortening of the Rh−Rh bonds in the trimers can be attributed to the nature of the molecular orbitals shown in Scheme 3. In the trimer, the originally nonbonding $1a_{2u}$ orbital is stabilized through mixing with the $2a_{2u}$ orbital. Consequently, in the trimer, two bonding and one antibonding molecular orbitals are filled, whereas in the dimer, one bonding and one antibonding molecular orbitals are occupied.

In the three salts, $([(C_6H_5CH_2NC)_{12}Rh^{V/III}_3I_2]I_3$, $[(C_6H_{11}NC)_{12}Rh^I_3][(C_6H_{11}NC)_{12}Rh^{V/III}_3Cl_2]Cl_6$, and $[(C_6H_{11}NC)_{12}Rh^{V/III}_3Cl_2][(C_6H_{11}NC)_8Rh^I_2][(C_6H_{11}NC)_4Rh^I]Cl_6 \cdot 16H_2O \cdot 3C_6H_6)$, which contain ions of the type $[(RNC)_{12}Rh^{V/III}_3Cl_2]^{3+}$, the Rh_3 unit is linear and the Rh−Rh distances, which fall in the range 2.75−2.79 Å, are shorter than the corresponding distances in the ions of the type $[(RNC)_{12}Rh^I_3]^{3+}$. Again, oxidation results in strengthening of the Rh−Rh bonding by removal of the two electrons in the antibonding $2a_{1g}$ orbital (see Scheme 3).

The dimeric ions, $[(RNC)_8Rh^I_2]^{2+}$, are unusual because usually they have a nearly eclipsed arrangement of the isocyanide ligands. These dimers include not only the one found in $[(C_6H_{11}NC)_{12}Rh^{V/III}_3Cl_2][(C_6H_{11}NC)_8Rh^I_2][(C_6H_{11}NC)_4Rh^I]Cl_6 \cdot 16H_2O \cdot 3C_6H_6$, which is shown in Figure 7, but also $[(C_6H_{11}NC)_8Rh^I_2]Cl_2 \cdot 0.5C_6H_6 \cdot 2H_2O$,[15] as well as $[(p\text{-}FC_6H_4NC)_8Rh^I_2]Cl_2 \cdot H_2O$[14] and $[(p\text{-}O_2NC_6H_4NC)_8Rh^I_2]Cl_2$.[14] In contrast, ions of the types $[(RNC)_8Rh^I_2X_2]^{2+}$, $[(RNC)_{12}Rh^I_3]^{3+}$, and $[(RNC)_{12}Rh^I_3X_2]^{3+}$ all have nearly staggered arrangements of their ligands, as does one example of the $[(RNC)_8Rh^I_2]^{2+}$ class, $[(PhNC)_8Rh^I_2]^{2+}$.[12] The staggered arrangement of the ligands in these complexes certainly minimizes steric interactions between the ligands and facilitates close interactions between the rhodium ions. The eclipsed arrangement found in most of the $[(RNC)_8Rh^I_2]^{2+}$ dimers may also be a factor responsible for the fact that the Rh−Rh distances in these dimers are longer than the corresponding distances in the closely related but staggered trimers, $[(RNC)_{12}Rh^I_3]^{3+}$. In the eclipsed arrangement, ligand−ligand interactions may also make a significant contribution to the dimer stability, as noted in a computational study of metal−metal interactions in d^8 complexes.[34]

In conclusion, we reiterate a point made previously. When multiple equilibria are occurring in solution, a variety of different chemical entities can crystallize as we have shown here with $[(C_6H_{11}NC)_4Rh^I]^+$. In this case, systematic variation of the anion, solvent, and ligand substituents allowed isolation of a number of chemically distinct complexes, as well as mixed crystals containing two or three distinct cations. Development of combinational approaches to crystallization, such as the one recently reported by Grzesiak and Matzger for polymorph generation,[6] also hold promise in studying solutions where multiple equilibria are involved.

(33) Prater, M. E.; Pence, L. E.; Clérac, R.; Finniss, G. M.; Campana, C.; Auban-Senzier, P.; Jérome, D.; Canadell, E.; Dunbar, K. R. *J. Am. Chem. Soc.* **1999**, *121*, 8005.

(34) Novoa, J. J.; Aullón, G.; Alemany, P.; Alvarez, S. *Inorg. Chem.* **1995**, *117*, 7169.

Experimental Section

Materials. Samples of $[(C_6H_{11}NC)_4Rh^{I}]Cl$, $[(C_6H_{11}NC)_{12}Rh^{I}_3](AsF_6)_3$, $[(C_6H_{11}NC)_{12}Rh^{I}_3](SbF_6)_3$, and $[(C_6H_{11}NC)_4Rh^{I}](BPh_4)$ were obtained by established routes.[12,35]

Crystal Growth. $[(C_6H_{11}NC)_8Rh^{II}_2Cl_2](BF_4)_2$. The green solid $[(C_6H_{11}NC)_4Rh^{I}]Cl$ (57.7 mg) was placed in a 25 mL Erlenmeyer flask and dissolved in 10 mL of deionized water to produce a purple solution. A 64.9 mg sample of $(NH_4)_2SnF_6$ was added to the purple solution. The solution was stirred for 1 h. The color of the solution changed from purple to yellow in 20 min. The aqueous solution was then filtered into a 50 mL Erlenmeyer flask containing 503.4 mg of NH_4BF_4 dissolved in water. This yellow solution was stirred in air without heating for an hour. The yellow precipitate was collected by filtration and washed with a minimum volume of water: yield, 33 mg (48.9%). Straw yellow crystals suitable for single-crystal X-ray diffraction were obtained by following the same procedure but omitting any stirring in the final step.

$[(C_6H_{11}NC)_{12}Rh^{I}_3](AsF_6)_3$. A mixture of 92.1 mg of $[(C_6H_{11}NC)_{12}Rh^{I}_3](AsF_6)_3$ and 5.0 mL of ethanol was heated in a 25 mL Erlenmeyer flask until a red-orange solution formed. The solution was cooled to room temperature and allowed to slowly evaporate. After 4 days, green crystalline blocks of the product were harvested (yield, 54%) and used for the crystallographic study.

$[(C_6H_{11}NC)_{12}Rh^{I}_3](SbF_6)_3$. Green plates were obtained in 67% yield by the method used for the crystallization of $[(C_6H_{11}NC)_{12}Rh^{I}_3](AsF_6)_3$.

Green Plates of $[(C_6H_{11}NC)_{12}Rh^{V/III}_3Cl_2][(C_6H_{11}NC)_{12}Rh^{I}_3]Cl_6$, Brown Plates of $[(C_6H_{11}NC)_{12}Rh^{V/III}_3Cl_2][(C_6H_{11}NC)_4Rh^{I}]_3Cl_6\cdot 16H_2O\cdot 3C_6H_6$, and Red-Orange Cubes. A sample of 0.6 mL of cyclohexyl isocyanide was added to solution of 0.3324 g of (1,5-cyclooctadiene)$_2Rh_2(\mu\text{-}Cl)_2$ in 15 mL of benzene. The sample was stirred for 2 h and filtered to remove a yellow precipitate. The red filtrate was transferred to 5 mm glass tubes and carefully layered with diethyl ether or with cyclohexane. Visual inspection revealed the growth of three different types of crystals. Red-orange cubes, the major product, grew in the benzene layer, while green crystals of $[(C_6H_{11}NC)_{12}Rh^{III/V}_3Cl_2][(C_6H_{11}NC)_{12}Rh^{I}_3]Cl_6$ grew in 24% yield in the ether or cyclohexane layer. Brown crystals of $[(C_6H_{11}NC)_{12}Rh^{V/III}_3Cl_2][(C_6H_{11}NC)_8Rh^{I}_2][(C_6H_{11}NC)_4Rh^{I}]Cl_6\cdot 16H_2O\cdot 3C_6H_6$ formed 4% yield at the solvent/anti-solvent interface.

Physical Measurements. Infrared spectra were recorded as neat powders on a Mattson Genesis II FT-IR spectrometer fitted with a Specac ATR accessory. Electronic absorption spectra were recorded using a Hewlett-Packard 8450A diode-array spectrophotometer.

X-ray Crystallography and Data Collection. The crystals were removed from the glass tubes in which they were grown together with a small amount of mother liquor and immediately coated with a hydrocarbon oil on the microscope slide. Suitable crystals were mounted on glass fibers with silicone grease and placed in the cold dinitrogen stream of a Bruker SMART Apex II diffractometer with graphite-monochromated Mo Kα radiation at 90(2) K. Crystal data are given in Table 1. The structures were solved by direct methods and refined using all data (based on F^2) using the software of SHELXTL 5.1. A semiempirical method utilizing equivalents was employed to correct for absorption.[36] Hydrogen atoms were located in a difference map, added geometrically, and refined with a riding model.

Acknowledgment. We thank the Petroleum Research Fund (Grant No. 37056-AC) for support and the Tyco Foundation for a fellowship for J.R.S.

Supporting Information Available: X-ray crystallographic files in CIF format for $[(C_6H_{11}NC)_{12}Rh^{I}_3](SbF_6)_3$, $[(C_6H_{11}NC)_{12}Rh^{I}_3](AsF_6)_3$, $[(C_6H_{11}NC)_8Rh^{II}_2](BF_4)_2$, $[(C_6H_{11}NC)_{12}Rh^{V/III}_3Cl_2][(C_6H_{11}NC)_{12}Rh^{I}_3]Cl_6$, and $[(C_6H_{11}NC)_{12}Rh^{V/III}_3Cl_2][(C_6H_{11}NC)_8Rh^{I}_2][(C_6H_{11}NC)_4Rh^{I}]Cl_6\cdot 16H_2O\cdot 3C_6H_6$. This material is available free of charge via the Internet at http://pubs.acs.org.

IC7008013

(35) Dart, J. W.; Lloyd, M. K.; Mason, R.; McCleverty, J. A. *J. Chem. Soc., Dalton Trans.* **1973**, 2039.

(36) *SADABS 2.10*, Sheldrick, G. M. based on a method of Blessing, R. H. *Acta Crystallogr., Sect. A* **1995**, *A51*, 33.